**Carcinogenesis** vol.35 no.8 pp.1807–1813, 2014
doi:10.1093/carcin/bgu100
*Advance Access publication April 28, 2014*

# A critical role of non-classical MHC in tumor immune evasion in the amphibian *Xenopus* model

**Nikesha Haynes-Gilmore[1,2], Maureen Banach[1], Eva-Stina Edholm[1], Edith Lord[1] and Jacques Robert[1,*]**

[1]Department of Microbiology and Immunology and [2]Department of Pathology, University of Rochester Medical Center, Rochester, NY 14642, USA

*To whom correspondence should be addressed. Department of Microbiology and Immunology, University of Rochester Medical Center, 601 Elmwood Avenue, Box 672, Rochester, NY 14642, USA. Tel: +585 275 1722; Fax: +585 473 9573;
Email: jacques_robert@urmc.rochester.edu

**Non-classical class Ib (class Ib) genes are found in all jawed vertebrates, including the amphibian *Xenopus*, which possesses at least 20 distinct *Xenopus* non-classical *c*lass Ib genes (XNCs). As an immune evasion strategy, tumors often downregulate surface expression of classical major histocompatibility complex class Ia molecules. In contrast, cancers commonly express class Ib molecules, presenting an alternative for tumor immune recognition. We characterized a novel XNC, XNC10, functionally similar to CD1d from a class Ia-deficient thymic lymphoid tumor (15/0), which grows aggressively in *Xenopus* LG-15 cloned animals. To investigate the roles of XNC10 in antitumor immunity, we generated stable 15/0-transfectants with silenced XNC10 mRNA and protein expression. Notably, XNC10 silencing resulted in acute tumor rejection by naturally class Ia-deficient syngeneic tadpoles, with greater potency of rejection in tumors with more efficient XNC10 knockdown. *In vivo* killing assays shows that the rejection of XNC10-deficient tumors is due to a cell-mediated cytotoxic immune response elicited by the tadpole host. Importantly, priming enhances XNC10-deficient tumor rejection. Flow cytometry reveals that XNC10-deficient tumor rejection is associated with an accumulation of XNC10-restricted invariant T cells and conventional CD8 T cells as well as other leukocytes. Similarly, semisolid tumor grafts in tadpoles also exhibit leukocytes infiltration. These findings suggest that XNC10 allows the 15/0-tumor to escape immune recognition and class Ia-independent cytotoxicity, thus emphasizing the critical roles of class Ibs in tumor immunity.**

## Introduction

Major histocompatibility complex (MHC) class Ia (class Ia) molecules play important roles in CD8 T cell-mediated recognition and elimination of tumors (1). However, in order to escape immune surveillance, and subsequent cell-mediated killing, tumor cells frequently downregulate surface expression of class Ia molecules, which correlate with poor prognosis and unfavorable patient outcome (1,2). Impaired class Ia expression has been reported for a wide variety of solid tumors including melanoma, colorectal, bladder, head and neck, breast, lung, kidney, prostate and cervical cancers (reviewed in ref. 3). In contrast to the decreased expression of class Ia molecules during tumorigenesis, cancer cells commonly overexpress non-classical MHC class Ib (class Ib) molecules (4–6). Class Ib genes are found in all jawed vertebrates, including the amphibian *Xenopus* and are structurally similar but functionally disparate compared to classical class Ia genes. Unlike class Ia, class Ib molecules usually have limited tissue distribution and low polymorphism. Moreover, class Ib expression is often an indicator of intracellular stress and/or malignancy (6–8). It has been proposed that class Ib overexpression may be used as an additional mechanism by which the tumor can escape immune surveillance (6). Even though mounting evidence suggests that class Ib molecules play critical roles in tumor immunity, these studies are often correlative and in some cases contradictory.

Some of the aberrantly expressed class Ibs in human tumors include HLA-E, HLA-G and HLA-F. For instance, HLA-E, which is abnormally expressed in human lymphoma, melanoma, ovarian cancer and glioblastoma, has immunosuppressive properties and also inhibits NK function in glioblastoma (9). Human metastatic melanoma has also been shown to express higher levels of HLA-G molecules when compared to the healthy tissue of the same patient (6). Additionally, it has been shown that HLA-F gene expression on B and T cells is upregulated upon cell activation leading to the binding of inhibitory receptors and that its expression is also a prognostic factor in non-small-cell lung cancer (10–12). Similarly, studies in mice have revealed that expression of the HLA-G functional analog Qa-2 can protect tumor cells from killing by NK cells and lymphokine-activated killer cells (13). Although the current model predicts that the absence of class Ia should trigger tumor-specific killing by NK cells, class Ia-deficient tumors still persist. Thus, it is plausible that the expression of class Ib molecules on tumor cells may prevent recognition and destruction of these cells by the immune system.

The amphibian *Xenopus* laevis is a unique model system ideally suited for investigating fundamental tumor immunity. The development and function of the immune system is remarkably well conserved between *Xenopus* and mammals. For example, frogs have thymus, spleen as well as thymic-educated T cells, B cells and RAG-mediated T- and B-cell-rearranged receptors (14). Unlike mammals, however, *X. laevis* have a single class Ia gene per genome. This class Ia gene is highly polymorphic and ubiquitously expressed in adults, whereas class Ia protein expression is inconsistent in tadpoles until the onset of metamorphosis. In addition, *X. laevis* possess at least 20 *Xenopus* non-classical class Ib genes (*XNCs*), which like their mammalian counterparts are oligomorphic and limited in tissue expression (15,16).

Notably, we have characterized a novel XNC, XNC10 from a spontaneously arising class Ia-deficient thymic lymphoid tumor (15/0), which grows aggressively in *Xenopus* LG-15 MHC compatible cloned animals (16). In healthy animals, XNC10 has a lymphoid-specific expression pattern; it is primarily expressed by thymocytes rather than on the thymic epithelium from early ontogeny and is essential for the differentiation of a distinct invariant T (iT) cell subpopulation (17). In addition, in contrast to mammals whose class Ib genes are rarely orthologous, XNC10 shows an unusually high degree of conservation in the Xenopodinae family (18). We hypothesized that in a class Ia-deficient tumor transplantation system, XNC10 provides immunoinhibitory signals. In this study, we have obtained evidence that the class Ib molecule XNC10 allows the 15/0 tumor to escape immune responses by preventing the recognition and killing by a subset of immune cells, thus underscoring the critical role that class Ib molecules play in tumor immune surveillance.

**Abbreviations:** APC, allophycocyanin; MHC, major histocompatibility complex; RT–PCR, reverse transcription–polymerase chain reaction; shRNA, short hairpin Ribonucleic acid; WT, wild type;XNCs, Xenopus non-classical class Ib genes.

## Materials and methods

### *Animals*

LG-15 *Xenopus*-cloned tadpoles were obtained from our breeding colony (http://www.urmc.rochester.edu/smd/mbi/xenopus/index.htm). All experiments were done with stage 54–55 (2-week-old) tadpoles. Animals were anesthetized by immersion in tricaine methanesulfonate (TMS; 0.1 g/l). All animals were handled under strict laboratory and UCAR regulations (Approval number 100577/2003–151) minimizing discomfort at all times.

### *Cell lines and stable transfections*

The naturally class Ia-deficient *Xenopus* 15/0 tumor cell line, was obtained from a spontaneously arising thymic tumor in a LG-15 cloned adult frog (19). Stable *Xenopus* 15/0 transfectants with silenced XNC10 expression were

© The Author 2014. Published by Oxford University Press. All rights reserved. For Permissions, please email: journals.permissions@oup.com

generated. A plasmid containing both a green fluorescent protein tag under the control of the human elongation factor 1 alpha promoter and a short hairpin RNA complementary to target sequence (gTA TTC AgT TgT AgC TTA) within XNC10 alpha-1 domain, under the control of the human U6 promoter was transfected into 15/0 wild-type (WT) tumor cells. At the same time, another plasmid containing a puromycin resistance gene as a selectable marker under the control of the *Xenopus* elongation factor 1 alpha promoter was co-transfected into the 15/0 WT tumor cells. Transfection was done using the Amaxa nucleofector kit V (Lonza) according to the manufacturer's instructions. Stable XNC10-deficient clones were selected by limited dilution in *Xenopus* cell culture media containing 2.5 µg/ml puromycin as previously described (20). Stable 15/0 transfectants containing scrambled short hairpin Ribonucleic acid (shRNA) also under the control of the U6 promoter were generated in parallel and by the same method as the XNC10-deficient clones. 15/0 tumor lines containing the consensus anti-XNC shRNA were described previously (16). For *in vitro* growth assays, 3× ($1 \times 10^5$) cells of either 15/0 WT, shXNC10 #4 or shXNC10 #7 were placed into a 96-well plate and allowed to grow at 27°C in a chamber containing a blood gas mix (5% $CO_2$, 21% $O_2$, 74% N). Cells were counted in triplicates at 24, 48 and 72 h.

*Reverse Transcription–Polymerase Chain Reaction (RT-PCR) and quantitative RT–PCR*

Total RNA was isolated using Trizol (Invitrogen) and 10 µg RNA was treated with DNase (Ambion, Life Technologies) according to manufacturer's instructions. To synthesize cDNA, 500 ng of DNase-treated RNA was used with the iScript cDNA synthesis kit (Bio-Rad) or oligo-dT, dNTPs, random hexamer primers and reverse transcriptase (Invitrogen). RT–PCR was then performed using 1 µl of cDNA template and 2× Taq master mix (Genescript Corp). Minus RT controls for DNA contamination were generated for each sample similarly to the cDNA synthesis described above, except that reverse transcriptase was excluded. Quantitative RT–PCR was performed using 2.5 µl of (1:3) diluted cDNA using the ΔΔCT method with the ABI7300 Real Time PCR system and PerfeCta SYBR Green FastMix ROX (Quanta Biosciences). All primers are listed in Supplementary Table S1, available at *Carcinogenesis* Online.

*Generation and characterization of anti-XNC10 antibodies*

To generate hybridoma secreting anti-XNC10 monoclonal antibodies, Line 1 (small-cell lung carcinoma) cells were transfected with the vector pcDNA3.1/myc-His(−) (Invitrogen) containing full length XNC10, and stable transfectants expressing the *X. laevis* recombinant XNC10 were selected. The Myc and His tags were used to detect the recombinant proteins expressed at the cell surface by flow cytometry, using fluorochrome-conjugated anti-Myc antibody Western blot analysis was also performed to detect recombinant protein. When stable transfectants expressing XNC10 was obtained, BALB/c mice were immunized by intraperitoneal injection of γ-irradiated tumor transfectants (21). Serum was taken 9–13 days after immunization and tested for reactivity by flow cytometry. To produce monoclonal antibodies, selected mice (with good reactivity against the antigen) were injected once intramuscularly with tumor transfectants, and their spleens were removed 20 days later for B cell fusion according to standard protocols (21,22). Hybridomas-producing monoclonal antibodies were screened by flow cytometry assays. Non-transfected line 1 cells were used as negative controls for western blot analyses.

The rabbit polyclonal anti-XNC10 antibody was generated by ProSci Inc., by immunization with an XNC10-specific peptide within the α1 region (TPSHSSFELYDDIEE, kindly provided by Dr. Patricia Simpson-Haidaris, University of Rochester, NY). The specificity of anti-XNC10 monoclonal antibody and antibody was determined by immunohistology, immunoprecipitation and western blot assays (Supplementary Figure S1, available at *Carcinogenesis* Online).

*Western blot assays*

15/0 tumor cell lines were lysed in RIPA buffer. Proteins (20 µg per lane) were separated on 10% polyacrylamide gels and transferred on PVDF membrane (Bio-Rad). After blocking with 10% BSA overnight at 4˚C, membranes were incubated with either anti-XNC10 291 monoclonal antibody supernatant or preabsorbed polyclonal anti-XNC10 (1:20 000 dilution), followed by secondary goat anti-mouse or rabbit HRP-conjugated antibody and developed by SuperSignal West Pico Chemiluminescence Substrate (Thermo Scientific). Band intensity was quantified using the Image J software. Preadsorbtion of anti-XNC10 rabbit antibody was performed on *Xenopus* red cells (XNC10-negative) twice for 1 h on ice.

*In vivo growth assays*

Tadpoles were intraperitoneally (IP) injected with $1 \times 10^5$ tumor cells of 15/0 WT, shScramble, shXNC10 #4 or #7 in 10 µl of amphibian phosphate-buffered saline. Peritoneal cells were collected 7 days posttransplantation by peritoneal lavage with 100 µl of amphibian phosphate-buffered saline as previously described (23). The volume obtained (90 ± 10 µl) was recorded. Peritoneal cells were counted using a hemocytometer and total numbers of cells retrieved per animal were calculated.

*Flow cytometry*

Peritoneal cells ($2.5 \times 10^5$ cells/per treatment) were stained with either 100 µl of undiluted hybridoma supernatant anti-CD5 (*Xenopus* pan T-cell marker, 2B1) or anti-*C*ortical *T*hymocyte antigen of *Xenopus* ([CTX]-tumor specific marker, X71) for 1 h at 4°C then washed with staining buffer (1% BSA in amphibian phosphate-buffered saline) then stained with 1:100 dilution of goat-anti-mouse allophycocyanin (APC) (Southern Biotech) for 30 min at 4°C. Cells stained with anti-CTX, were then incubated with either 0.5mg/ml *Xenopus*-specific biotinylated anti-CD8 (AM22) or MHC Class II (AM20) for 1h at 4°C followed by streptavidin-phycoerythrin (PE) (BD Pharmingen) for 30 min at 4°C. For staining with the class Ib XNC10 tetramer (XNC10-T), complexes were prepared as previously described in (17). Peritoneal cells ($2.5 \times 10^5$ cells/per treatment) were stained with 5 µg of XNC10-T-APC for 30 min at 4°C followed by incubation with monoclonal antibody CD8-FITC for 30 min at 4°C. Dead cells were excluded using Propidium Iodide (BD Pharmagen). All samples were washed and resuspended in 300 µl of staining buffer and examined by flow cytometry on a FACs Canto II instrument (BD Biosciences). Total number of invariant T (iT), CD8 T and Class II cells were calculated using cell counts and percentage of living cells, respectively. Fifty thousand events were collected gated for live cells and analyzed using the FlowJo software (Tree Star Inc.).

*Preparation of tumor-embedded collagen grafts*

To determine whether XNC10 deficiency results in tumor rejection, tumor cells were embedded in a collagen matrix. Accordingly, setting solution (10× Earle's Balanced Salt Solution + 0.2 M $NAHCO_3$ + 0.15 M NaOH) was added dropwise to rat tail collagen (BD Biosciences) on ice until the pH of the collagen was neutralized as previously described (24). Tumor cells (15/0 WT or shXNC10 deficient) were then mixed with the collagen solution at a concentration of $5 \times 10^5$ cells per 10 µl graft. Collagen/tumor mix was then pipetted into individual wells of 6-well plates and incubated at 27°C for 30 min to allow collagen polymerization. Two milliliters of either 15/0 WT media, previously described (21) was added to 15/0 WT collagen grafts and 15/0 WT media supplemented with 2.5 µg/ml puromycin was added to shXNC10-deficient tumor collagen grafts. Plates containing the grafts were then incubated at 27°C in chambers containing a blood gas mix (5% $CO_2$, 21% $O_2$, 74% N) until use.

*Tumor grafts*

Small subcutaneous incisions were made on anterior left or right dorsal surface of tadpoles, between the eye and the brain, and the collagen 15/0 tumor grafts of either WT or shXNC10#7 were inserted subcutaneously within the incisions so that each animal contained both WT (anterior left) and shXNC10#7 (anterior right) grafts. Digital Images were taken using an SMZ1500 Nikon stereo microscope and area of XNC10-deficient and WT grafts were obtained using ImageJ software. The area of XNC10-deficient grafts relative to WT grafts was then calculated for each animal.

*Histology*

A small incision was made on the anterior left or right region of the tadpole and the collagen-embedded tumor grafts were removed 7 days postgrafting. Grafts were briefly washed with amphibian phosphate-buffered saline, placed into cast containing Optimal Cutting Temperature compound (OCT) then frozen on dry ice. Serial 8 µM sections were taken and fifth section was stained with hematoxylin and eosin. Tumor collagen grafts were allowed to grow for 3 weeks when ascites fluid was removed and placed onto slide by cytospin and then stained with Giemsa as previously described (25). Slides were examined using an Axiovert 200 inverted microscope and Infinity 2 digital camera (objective: 40/0.6, Zeiss).

*In vivo killing assays*

To discriminate between WT and XNC10-deficient tumor cells, 15/0 WT cells were stained with either 2 µM of the red fluorochrome PKH26 (PKH) (Sigma) or 40 µM of carboxyfluorescein succinimidyl ester (CFSE) (Invitrogen) and 15/0 shXNC10 #7 cells were stained with 40 µM CFSE according to manufacturer's instructions. Five hundred thousand cells at a 1:1 ratio of either WT-PKH:WT-CFSE or WT-PKH:shXNC10#7CFSE were transplanted into the peritoneum of LG-15 tadpoles. Cell mixtures were analyzed by flow cytometry at day 0 prior to transplantation. At distinct times (2, 3 and 7 days) posttransplantation cells were removed by peritoneal lavage and examined by flow cytometry (FACs Canto II, BD Biosciences) and results analyzed in Flow Jo (Tree Star Inc.). Percent killing was calculated by determining the differences between the PKH+ and CFSE+ populations on days 2, 4 and 7 from day 0 and expressed as percentages.

*Statistical analysis*

All quantitative data were analyzed using a one-way ANOVA and the Vassar Stat software (www.vassarstats.net).

## Results

*Generation of XNC10-deficent 15/0 cell lines*

To delineate the roles of non-classical MHCs in tumor immunity, we examined the tumor-associated *Xenopus* class Ib molecule, *XNC10* in the context of the 15/0 lymphoid tumor model. In normal tissues, while low levels of XNC10 expression are detected in liver, gills, kidneys and spleen, *XNC10* is clearly predominantly expressed in the thymus of both tadpoles (Figure 1A) and adults (15). Comparably, XNC10 gene expression in the 15/0 tumor cells is about 4-fold higher then that observed in tadpole thymus suggesting a putative role of XNC10 in immunity to 15/0 tumors. To address this, we generated XNC10-deficent 15/0 tumor clones stably expressing an anti-XNC10 shRNA. Two distinct clones were selected exhibiting, respectively, ~60% (clone #4) and ~90% (clone #7) knockdown (KD) of *XNC10* expression, respectively, as determined by RT–PCR (Figure 1A) and quantitative RT–PCR (Figure 1B). Control cells transfected with a scramble shRNA had no significant changes of *XNC10* expression (Figure 1B and 1C). To confirm the specificity of the *XNC10* KD, we assessed the expression level of *XNC11*, which is the other *XNC* gene highly expressed by the 15/0 tumor cells (15). RT–PCR analysis showed no perturbation of *XNC11* gene expression (Figure 1A). The gene expression of the 15/0 tumor-specific marker, cortical thymocyte antigen (CTX) was also unaltered by *XNC10* KD (Figure 1A). Additionally, flow cytometry analysis revealed no significant differences in surface protein expression of CD5, CD8 and CTX on either WT, shScramble or shXNC10 #7 tumor cells (Supplementary Figure S2, available at Carcinogenesis Online). Importantly, effective XNC10 protein knockdown was further confirmed at the protein level by western blot analysis using either an XNC10-specific polyclonal antibody or a monoclonal antibody (Figure 1D and Supplementary Figure S1, available at *Carcinogenesis* Online).

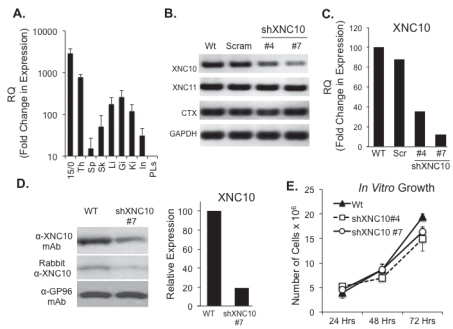


**Fig. 1.** XNC10 expression pattern and generation of stable XNC10-deficient 15/0 tumor cell lines. (**A**) XNC10 gene expression in normal tadpoles tissues and 15/0 tumor cells by qPCR. Th, thymus; Sp, spleen; Sk, skin; Li, liver; Gi, gills; Ki, kidney; In, intestine; PLs, peritoneal leukocytes. (**B**) 15/0 tumor cells were transfected with either a scrambled shRNA or an anti-XNC10 shRNA construct and stable clones were generated. RT–PCR gene expression analysis of XNC10, XNC11, CTX and GAPDH in 15/0 WT, shScramble, shXNC10 clone #4 and #7 tumor cells. (**C**) Quantitative RT–PCR gene expression analysis of XNC10 on 15/0 WT, shScramble, shXNC10 clone #4 and #7 tumor cells. (**D**) Western blot analysis of anti-XNC10 antibodies. Left: 15/0 WT and shXNC10#7 cell lysates incubated with the 291 monoclonal antibody (top) or rabbit polyclonal (bottom) anti-XNC10 antibodies. Left: Densitometry analysis of the XNC10 protein expression assessed using the 291 monoclonal antibody. (**E**) Assessment of tumor transfectants' proliferation; $1 \times 10^5$ cells of 15/0 WT, shXNC10 #4 or shXNC10 # were plated in triplicate and grown *in vitro* then cells were collected and counted 24, 48 and 72 h *later*. $n = 3$ independent experiments.

Finally, we assessed the effect of XNC10 silencing on tumor cell proliferation *in vitro* cell culture. *In vitro* growth of both XNC10-deficient clones (#4 and #7) was not significantly different compared to WT or shScramble15/0 control cells, indicating that transfection and XNC10 KD did not have negative effects on tumor growth *in vitro* (Figure 1E).

*Silencing of endogenous XNC10 in 15/0 tumor cells results in tumor rejection by syngeneic naturally class Ia-deficient LG-15 larval hosts*

The poorly immunogenic 15/0 tumor grows aggressively in both LG-15 tadpoles and adults (19). In light of the high XNC10 expression in these cells, we reasoned that this molecule might facilitate immune evasion. To address this hypothesis, we introduced intraperitoneally WT, shScramble, shXNC10 #4 or shXNC10 #7 tumor cells into syngeneic LG-15 tadpoles and compared tumor growth. At 7 days postchallenge, cells from the peritoneum of individual tadpoles were harvested by peritoneal lavage. The fluid volumes retrieved (90 ± 10 µl) and the cell numbers were determined for each animal. Cells from the peritoneal cavity included both growing tumor cells and immune cells that infiltrated the peritoneal cavity. Significantly fewer total peritoneal cells were retrieved from animals transplanted with 15/0 shXNC10 #4 and #7 compared to WT with the greatest decrease observed in animals transplanted with clone #7 (Figure 2A).

To determine more accurately the effect of XNC10 deficiency on 15/0 tumor cell growth *in vivo*, peritoneal cells from 3–5 transplanted animals were pooled and stained for CTX, a maker with expression restricted to immature thymocytes and the 15/0 tumor (26). Interestingly, decreased numbers of total peritoneal cells retrieved from animals transplanted with the XNC10-deficient 15/0 cells (clones #4 and #7) correlated with diminished percentage and numbers of $CTX^+$ XNC10-deficient tumor cells, with almost no tumors found in shXNC10 #7 animals (Figure 2B and C and Supplementary Figure S3, available at *Carcinogenesis* Online). No accumulation of XNC10-deficient 15/0 cells in other tissues such as spleen, liver and kidneys was detected (data not shown) ruling out a possible egress of XNC10-deficient tumors outside the peritoneal cavity.

To obtain further evidence that *XNC10* deficiency results in tumor rejection, we developed a semisolid tumor approach by embedding 15/0 tumor cells into a collagen matrix. We grafted the semisolid tumor dorsally and bilaterally onto single LG-15 tadpoles under the skin. Notably, the transparency of *Xenopus* tadpoles permits the direct visualization and hence easy monitoring of tumor growth. Animals

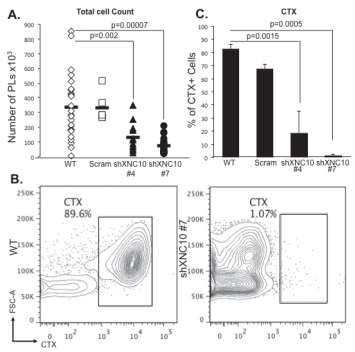


**Fig. 2.** XNC10-deficient 15/0 tumor cells are rejected by syngeneic LG-15 larval hosts. (**A**) LG-15 tadpoles were intraperitoneally injected with $1 \times 10^5$ 15/0 WT, shScramble, shXNC10 clone #4 or #7 tumor cells and peritoneal exudates were collected and total cells from individual animals were counted 7 days posttransplantation. (**B** and **C**), Total peritoneal cells retrieved from 15/0 WT, shScramble, shXNC10 clone #4 or #7 tumor-transplanted recipients were combined into respective groups and stained with anti-CTX-APC. (B) Representative flow cytometry scatter plots of anti-CTX-APC of 15/0 WT and shXNC10#7 transplanted animals. (C) Quantification of CTX+ tumor cells in WT, shScramble, shXNC10 clone #4 or #7 transplanted animals. $n = 4$ independent experiments, with 3–5 animals per experiment.

grafted with WT and XNC10-deficient tumors, on opposite sides, displayed pronounced WT tumor burden, whereas XNC10-deficient tumors failed to grow (Figure 3A). Similar results were obtained in several independent experiments where the growth of the XNC10-deficient tumors was markedly reduced compared to WT 15/0 (Figure 3B). Even when tumor engraftment was prolonged for 2 months, XNC10-deficient tumors failed to develop and upon necropsy no tumor cells were found in the graft (data not shown). Furthermore, histological analysis at 7 days postengraftment revealed establishment and growth of 15/0 WT tumors (Figure 3C I–II, left panel), while in contrast collagen grafts initially containing XNC10-deficient tumors were strikingly devoid of tumor cells, albeit containing some immune cell infiltration (Figure 3C III–IV, right panel).

### *Transplantation of XNC10-deficient 15/0 tumor elicits cellular antitumor immune responses*

To determine whether the rejection of transplanted XNC10-deficient tumors was due to a specific immune response, we examined the composition of peritoneal leukocyte exudates following transplantation of XNC10-deficient and control tumors. Accordingly, we performed flow cytometry analysis using *Xenopus*-specific monoclonal antibodies recognizing MHC class II (only expressed on macrophages, neutrophils and B cells in tadpoles), CD8 and CD5 (*Xenopus* pan-T-cell marker) as well as CTX to distinguish 15/0 tumors. Compared to WT 15/0 peritoneal exudates containing marginal leukocyte infiltration, there was significant accumulation of CTX-negative $CD8^+$ T cells (Figure 4A and Supplementary Figure S4B, available at *Carcinogenesis* Online), $CD5^+$ total T cells (Supplementary Figure S4A, available at *Carcinogenesis* Online) and MHC class $II^+$ cells (Figure 4B and Supplementary Figure S4C, available at *Carcinogenesis* Online) following transplantation of XNC10-deficient 15/0 # 4 and #7 clones. Furthermore, infiltration of CTX-negative T cells and CTX class II leukocytes was more pronounced in animals transplanted with clone #7 that exhibited greater XNC10 knockdown.

To substantiate that leukocyte cell infiltration resulted from XNC10 deficiency by 15/0 tumors we also analyzed peritoneal cells from tadpoles transplanted with 15/0 shScramble controls as well as 15/0 stably transfected with a vector expressing a puromycin resistant gene. As in the case of WT 15/0 tumors, these transfectants bearing normal expression of XNC10 induced only minimal leukocyte infiltration (Figure 4 and Supplementary Figure S4B and C, available at *Carcinogenesis* Online).

Giemsa staining of cells isolated from semisolid grafts also revealed substantially more granulocytes and macrophages within the XNC10-deficient tumor grafts (Figure 4C III–VI) as compared to WT grafts (Figure 4C I–II) from the same individual animals.

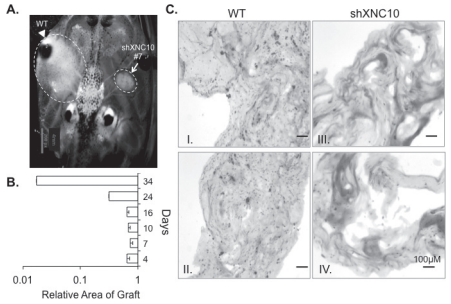


**Fig. 3.** XNC10 silencing compromises *in vivo* tumor growth in semisolid tumor grafts of syngeneic tadpoles. (**A**) Representative image of subcutaneous collagen grafts 7 days posttransplantation with either $5 \times 10^5$ 15/0 WT (left) or shXNC10#7 (right) tumor cells in LG-15 tadpoles. (**B**) Area of XNC10-deficient compared to WT tumor graft at 4, 7, 10, 16, 24 and 34 days posttransplantation. Three independent experiments were performed with 3–9 animals per group. (**C**) H&E staining of cryosections of tumor collagen grafts 7 days posttransplantation. WT grafts; left two panels (I and II) and shXNC10#7 tumor grafts; right two panels (III and IV).

Given that XNC10 is required for the differentiation and function of a subset of invariant T (iT) cells (18), we were interested in determining the abundance of these cells in the peritoneal fluid of growing WT and rejected XNC10-deficient tumor cells. Thus, we performed flow cytometry analysis using XNC10-tetramers (XNC10-T) (18). Interestingly, virtually no XNC10-restricted iT were detected in peritoneal exudates of naïve tadpoles (Figure 5A, first panel). In contrast, XNC10-restricted iT cells, mostly CD8 negative (type I), constituted a prominent fraction (between 10 and 20%) of PLs from LG-15 larvae 7 days following transplantation with WT or shXNC10#7 (Figure 5A and B). No difference in occurrence of putative type II ($XNC10\text{-}T^+/CD8^+$) iT cells was observed between tadpoles transplanted with WT or XNC10-deficient tumors (data not shown). There was a slight, but not statistically significant increase in the percentage of XNC10-restricted iT cells in peritoneal exudates from

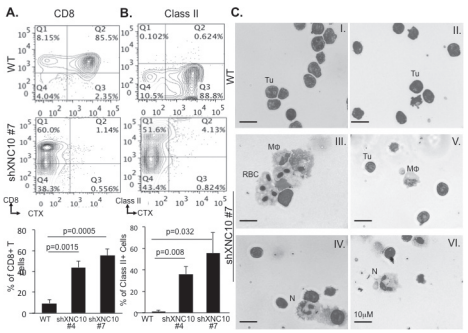


**Fig. 4.** XNC10-deficient 15/0 tumors elicit cellular antitumor immune responses. (**A** and **B**), Tadpoles were IP injected with $1 \times 10^5$ cells of either 15/0 WT, shScramble shXNC10 #4 or #7, cells were collected 7 days posttransplantation and each group pooled, immune-stained for CTX-APC, CD8-PE or MHC class II-PE and analyzed by flow cytometry. Percentage of (A) CTX–/CD8+ and (B) CTX-/Class II+ cells was determined. Top panels depict representative flow cytometry scatter plots of WT and shXNC10 #7. Three independent experiments with five animals per group were performed (**C**), Giemsa stain of cells isolated after 2 weeks of *in vivo* growth from WT collagen grafts (I and II) and XNC10-deficient tumor grafts (III and IV); tumor cells (Tu), macrophages (MΦ) and neutrophils (N).

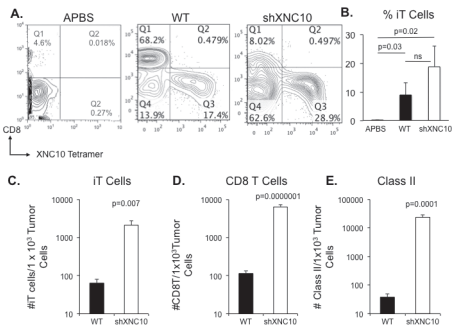


**Fig. 5.** Differential immune cell recruitment within tadpole peritoneum following WT and XNC10-deficient tumor cell transplantation. Tadpoles were IP injected with $1 \times 10^5$ WT or shXNC10 #7 15/0 tumor cells, whereas control animals were injected with an equal volume of amphibian phosphate-buffered saline. Peritoneal cells were collected 7 days posttransplantation and counted for each individual. Cells for each group were then pooled, immune-stained for XNC10-T-APC and CD8-FITC and analyzed by flow cytometry. Dead cells were excluded using propidium iodide. (**A**) Representative flow plots showing XNC10-T-APC- and CD8-FITC-stained peritoneal exudates from amphibian phosphate-buffered saline, WT and XNC10-deficient transplanted animals. (**B**) Percent of iT cells calculated for each individual. Total number of C, iT; D, CD8 and E, Class II per 1000 tumor cells was determined for both WT and XNC10-deficient peritoneal exudates. Three independent experiments with give to eight animals per group were performed. *P*-values indicated within each histogram were determined using One way ANOVA (B) or Student's *t*-test (**C**–**E**).

animals transplanted with XNC10-deficient compared to WT tumor cells (Figure 5B), with a total number of ~$2 \times 10^4$, iT cells in peritoneal exudates of WT and ~$7 \times 10^3$ iT cells in shXNC10 #7 transplanted animals. However, when the tumor cell number (determined as CTX positive cells) were taken into account, there was significantly more iT cells (Figure 5D), as well as more CD8 (Figure 5E) and Class II$^+$ (Figure 5F) cells per tumor cell in peritoneal exudates of animals transplanted with XNC10-deficient tumor cells.

Collectively, these data suggest that 15/0 lymphoid tumors deficient for the class Ib, XNC10, exhibit increased immunogenicity and induce more potent host cellular immune responses.

### *XNC10-deficient tumors are rejected by cell-mediated cytotoxic responses*

To determine whether the rejection of XNC10-deficient tumor cells was due to cell-mediated cytotoxicity, we modified a *Xenopus in vivo* killing assay (27). To conveniently discriminate 15/0 WT tumor from XNC10-deficient tumor by flow cytometry, the cells were labeled with red (PKH) and green (CFSE) fluorochromes. Thus, 15/0 WT tumor cells were labeled with either 2 µM PKH or 40 µM CFSE (15/0 WT-PKH or 15/0 WT-CFSE) and 15/0 XNC10-deficient tumor cells were labeled with 40 µM CFSE (15/0 shXNC10-CFSE). A 1:1 mixture of 15/0 WT-PKH:15/0 WT-CFSE and 15/0 WT-PKH:15/0 shXNC10-CFSE were intraperitoneally transplanted into LG-15 tadpole recipients and peritoneal cells were collected at 2, 4 and 7 days posttransplantation. We determined the proportion of PKH to CFSE cells using flow cytometry analysis and calculated percentage rejection. In several independent experiments, the XNC10-deficient cells were preferentially killed (70% by day 7), whereas in stark contrast the WT cells continued to grow actively within tadpole hosts (Figure 6). Although CFSE staining decreased along with tumor cell division, positive signal was still clearly detectable at 7 days posttransplantation for WT 15/ cells, but almost undetectable for XNC10-deficient 15/0 tumor cells (Figure 6A). Cell numbers calculated using cell percentage obtained by flow cytometry further indicate that XNC10-deficient tumor cells are actively rejected (Figure 6C). Furthermore, CFSE dilution over the time posttransplantation is very similar between transplanted WT and XNC10-deficient tumor cells, which strongly argue against a growth defect resulting form XNC10 deficiency (Supplementary Figure S5, available at *Carcinogenesis* Online).

In accordance with our observations that within 7 days of transplantation, shXNC10 #7 tumor cells undergo 99% killing, accompanied by robust immune responses (Figures 2C and 4), we primed tadpoles with XNC10-deficient cells 7 days prior to performing *in vivo* killing assays to determine whether these responses were XNC10-specific and could be accelerated upon re-challenge. Indeed, XNC10-deficient tumor-primed animals rejected 70% of the XNC10-deficient tumors within16 h posttransplantation (Figure 7A). Notably, the complete elimination of XNC10-deficient tumors from unprimed animals requires 7 days (Figure 6). Interestingly, priming of animals with lethally irradiated 15/0 WT cells failed to induce killing *in vivo* 20 h posttransplantation (Figure 7B). Importantly, in addition to providing compelling evidence that XNC10 is critical for activation of cell-mediated immune rejection, the priming experiment rules out the possibility that XNC10 deficiency induces a growth defect of 15/0 tumor *in vivo*.

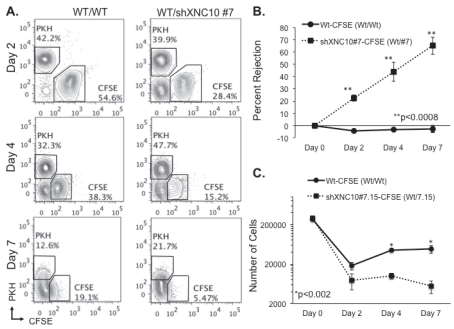


**Fig. 6.** XNC10-deficient tumors elicit, and are rejected by, cell-mediated cytotoxic responses. $5 \times 10^5$ cells at a 1:1 ratio of WT-PKH/WT-CFSE or WT-PKH/shXNC10 #7-CFSE were injected into LG-15 tadpoles. (**A**) Representative flow cytometry plots of cells harvested from individual tadpoles at 2, 4 and 7 days posttransplantation. (**B**) Calculated percent rejection from individual tadpoles of WT-CFSE and shXNC10#7-CFSE tumors 2, 4 and 7 days posttransplantation. (**C**) Number of WT-CFSE and shXNC10#7-CFSE cells injected (day 0) and retrieved from individual tadpoles at 2, 4 and 7 days posttransplantation. One representative experiment shown where $n$ = 6–8 animals.

## Discussion

Here we report that, in the amphibian *Xenopus*, the non-classical class Ib molecule, XNC10, is necessary for the immune evasion of the thymic-derived 15/0 tumors. The inhibitory roles of distinct tumor-expressed class Ib molecules have been described in detail *in vitro* (6,28). However, the precise mechanisms of class Ib interactions with antitumoral immune effectors *in vivo* is still not well established. Typically, class Ib genes display little homology or orthology among distinct vertebrate species. Notably, *XNC10* represents a unique class Ib monogenic lineage that is divergent from other class Ib genes, yet highly conserved across *Xenopus* species (17). In addition, *XNC10* gene orthologs of two evolutionarily distant *Xenopus* species, *X. laevis* and *X. tropicalis* share the same expression pattern with a predominant and developmentally early thymocyte expression, from the onset of thymic organogenesis, which suggests that these molecules have similar conserved functions (19). Moreover, XNC10 function in *X. laevis* is required for the development of a prominent iT cell subset reminiscent of CD1-restrcited iNKT cells (18). Thus, studying the functionally conserved roles of a class Ib molecule in alternative animal model systems serves to expand our understanding of the complex roles of class Ib molecules in tumor biology. In this regard, the functionally conserved *X. laevis* class Ib gene *XNC10* examined in the context of the MHC matched tadpole tumor transplantation model provides an innovative platform by which the complexity of tumor–class Ib interactions can be delineated.

As is the case with mammalian class Ia-deficient tumors expressing high level of class Ib molecules, the poorly immunogenic *Xenopus* 15/0 tumor (29) also exhibits elevated expression of the class Ib XNC10 compared to healthy tissues (Figure 1A) (14). We show in the present study that loss of *XNC10* function results in abrogated 15/0 tumor growth within the tadpole peritoneum. Notably, in addition to XNC10, the 15/0 tumor cells also express other class Ib molecules,

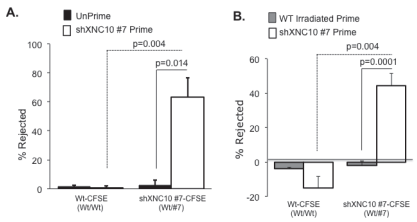


**Fig. 7.** Cytotoxic cell-mediated rejection of XNC10-deficient tumor cells is specific and long lasting. (**A**) Animals were either primed with $1 \times 10^5$ cells of viable shXNC10 #7 for 7 days or left unprimed and then transplanted with $5 \times 10^5$ cells at a 1:1 ratio of WT-PKH/WT-CFSE or WT-PKH/shXNC10#7-CFSE. Percent tumor rejection from individual tadpoles of WT-CFSE and shXNC10#7-CFSE for both primed and unprimed animals 16 h posttransplantation is shown. Representative experiment depicted, $N$ = 6 animals. (**B**) Animals were either primed with $1 \times 10^5$ cells of either lethally irradiated 15/0 WT or viable shXNC10 #7 for 7 days then transplanted with the 1:1 labeled WT/XNC10-deficient tumors. Percent tumor rejection from individual tadpoles of WT-CFSE and shXNC10#7-CFSE 20 h posttransplantation is shown. Representative experiment depicted, $n$ = 6 animals.

chiefly amongst them XNC11 (27). Provided that the frog *XNC11* gene expression profiles are distinct from XNC10, it stands to reason that these respective molecules have distinct roles. Possibly, in the absence of XNC10 molecules and hence the loss of the inhibitory signal, XNC11 molecules may facilitate immune recognition of these tumors. It will be interesting to determine the precise roles of other tumor-expressed class Ib molecules to better understand the balance between tumor immune recognition and evasion.

The increased expression of class Ib molecules during tumorigenesis renders them ideal targets for immunotherapy. Previous studies have revealed strikingly opposing roles of these molecules in cancer. In this regard, the elevated surface expression of a specific class Ib (e.g., XNC10) on primary tumors may confer an inhibitory signal (presumably) to a subset of immune cells, thereby facilitating tumorigenesis. Akin to our findings, others have also demonstrated immunoevasive roles for mammalian class Ib molecules (9,13). Intriguingly, the downregulation of the class Ib, CD1d molecules (normally highly expressed in healthy breast tissue) in highly metastatic breast tumors results in spontaneous breast cancer metastasis and decreases iNKT cytotoxicity toward these tumors (30). Additional murine studies have shown that the mouse class Ib Q9 molecule confers immune protection against metastatic melanoma outgrowth (31). Furthermore, our previous findings indicate that decreasing the expression of all tumor-expressing XNCs (using a shRNA targeting a consensus sequence shared by all XNCs) does not reverse the 15/0 tumor inhibitory phenotype (16). This underlines the putative duality of XNC molecules in support of our hypothesis that where some molecules, such as XNC10 may confer immunoinhibitory signals, others (possibly XNC11) may serve as immune-activating molecules. This idea would reconcile the discrepancies seen between the roles of distinct the class Ib molecules in tumor immunity, whereas it seems likely that similar to our model, distinct class Ib molecules either negatively or positively control tumor immune recognition. Elucidating the consequences of the varying surface class Ibs expression in the complex tumor–immune interactions will be pivotal to developing superior cancer therapies.

This manuscript represents the first report of tumor-specific killing in the naturally class Ia-deficient tadpole model system. Intriguingly, XNC10 deficiency resulted in not only robust immune infiltration into the tumors but also culminated in potent specific rejection of XNC10-deficient tumors. Indeed, the transplantation of both WT and XNC10-deficient tumors into individual animals resulted in specific elimination of only the XNC10-deficient tumors. This suggests that the immune effector cells responsible for this tumoricidal activity can discriminate, target and kill cells lacking XNC10. Keeping in mind that *Xenopus* is a poikilothermic vertebrate where consequently immune infiltration kinetics are typically slower than in homeotherms, unprimed animals kill more than 70% of the XNC10-deficient tumors in 7 days. Strikingly, XNC10-deficient tumor-primed animals exhibit faster and more robust XNC10-specific cytotoxic immune response, killing more than 70% of XNC10-deficient tumors in only 16 h posttransplantation. Priming against XNC10-deficient tumor also rules out the possibility that XNC10 deficiency results in a growth defect of 15/0 tumors *in vivo*.

Our previous *Xenopus* adult studies demonstrated that lethal irradiation of the WT 15/0 tumors only delayed the time to onset of growth of viable 15/0 WT tumors but did not inhibit tumor formation of these tumors (29). Here we show that akin to *Xenopus* adults, priming of tadpoles with irradiated 15/0 WT cells failed to enhance tumor rejection, irrespective of the status of XNC10. This confirms the general non-immunogenic properties of these wild-type 15/0 tumors and underlines the necessity of XNC10 to maintain this tumor phenotype.

We have recently identified a subpopulation of type I and type II XNC10-restricted iT cells with similarities to mammalian CD1d-restricted iNKT cells (17). In mammals, NKT cells have been shown to play dual roles in tumorigenesis by balancing the immunoregulatory axis through regulation by Type I iNKT and Type II NKT cells (reviewed in ref. 32). Type I iNKT cells have been shown to promote antitumor immune responses (33), whereas Type II NKT cells are pro-tumorigenic through the inhibition of CD8 T-cell-mediated lysis and by the activation of immunosuppressive cells such as MDSCs and Tregs (reviewed in ref. 32). Our data showing that XNC10-deficient tumor cells elicit antitumor immune response leading to their rejection suggest the involvement of type I iT cells. Indeed, using XNC10 tetramers a prominent fraction of CD8-negative (type I) iT cells are detected in peritoneal exudates from tadpoles transplanted with either WT or XNC10-deficient tumors but not from untreated tadpoles. Notably, the relative number of iT cells to tumor cells was significantly higher in 15/0 XNC10-deficient tumor cells compared to WT 15/0 tumor cells. Although type II XNC10T$^+$/CD8$^+$ were rare and not significantly changed between tadpoles challenged with WT or XNC10-deficient 15/0 tumors, it is plausible that the iT immunoregulatory axis may be modulated by changes in XNC10 expression as well as various chemokine and cytokines, thereby leading to tumor rejection. In humans, clinical trials using alpha-Gal-Cer to activate iNKT cells has had limited success thus far. This has been attributed to a variety of factors including the artificial stimulation of these iT cells. Our data suggest a natural alternative to stimulate type I iT cells by the manipulation of certain class Ibs thus shifting the balance away from tumor suppressive phenotype hence creating an avenue for successful immunotherapies.

Our findings underline the functional importance of the class Ib XNC10 in 15/0 tumor immune evasion and syngeneic host cell-mediated cytotoxicity. This article presents both an alternative model for studying the as-of-yet poorly defined roles of class Ib molecules in tumor immunity and offers an intriguing fundamental example of a mechanism by which tumor expression of these molecules may dictate antitumor responses. We believe that further investigation into the specific biological roles of class Ib molecules will pave the way toward the development of the next generation of cancer therapies.

## Supplementary material

Supplementary Table S1 and Figures S1–S5 can be found at http://carcin.oxfordjournals.org/

## Funding

This research was supported by the National Institutes of Health Grant (R24-AI-059830); a University of Rochester Wilmot Cancer Center Seed grant (E.-S.E.); a Kesel Fund Award (20115123 to N.H.).

## Acknowledgements

We would like to thank David Albright and Tina Martin for the expert animal husbandry and Dr Leon Grayfer, for discussions and critical reading of the manuscript and Dr Patricia Simpson-Haidaris for help with XNC10-specific peptide design.

*Conflict of Interest Statement:* None declared.

## References

1. Chang,C.C. *et al*. (2003) HLA class I defects in malignant lesions: what have we learned? *Keio J. Med*., **52**, 220–229.
2. Connor,M.E. *et al*. (1990) Loss of MHC class-I expression in cervical carcinomas. *Int. J. Cancer*, **46**, 1029–1034.
3. Bukur,J. *et al*. (2012) The role of classical and non-classical HLA class I antigens in human tumors. *Semin. Cancer Biol.*, **22**, 350–358.
4. de Kruijf,E.M. *et al*. (2010) HLA-E and HLA-G expression in classical HLA class I-negative tumors is of prognostic value for clinical outcome of early breast cancer patients. *J. Immunol.*, **185**, 7452–7459.
5. Goncalves,M.A. *et al*. (2008) Classical and non-classical HLA molecules and p16(INK4a) expression in precursors lesions and invasive cervical cancer. *Eur. J. Obstet. Gynecol. Reprod. Biol.*, **141**, 70–74.
6. Paul,P. *et al*. (1998) HLA-G expression in melanoma: a way for tumor cells to escape from immunosurveillance. *Proc. Natl Acad. Sci. USA*, **95**, 4510–4515.
7. Gleimer,M. *et al*. (2003) Stress management: MHC class I and class I-like molecules as reporters of cellular stress. *Immunity*, **19**, 469–477.

8. Ugurel,S. *et al*. (2001) Soluble human leukocyte antigen–G serum level is elevated in melanoma patients and is further increased by interferon-alpha immunotherapy. *Cancer*, **92**, 369–376.
9. Wolpert,F. *et al*. (2012) HLA-E contributes to an immune-inhibitory phenotype of glioblastoma stem-like cells. *J. Neuroimmunol.*, **250**, 27–34.
10. Ishitani,A. *et al*. (2006) The involvement of HLA-E and -F in pregnancy. *J. Reprod. Immunol.*, **69**, 101–113.
11. Lepin,E.J. *et al*. (2000) Functional characterization of HLA-F and binding of HLA-F tetramers to ILT2 and ILT4 receptors. *Eur. J. Immunol.*, **30**, 3552–3561.
12. Lin,A. *et al*. (2011) HLA-F expression is a prognostic factor in patients with non-small-cell lung cancer. *Lung Cancer*, **74**, 504–509.
13. Chiang,E.Y. *et al*. (2002) The nonclassical major histocompatibility complex molecule Qa-2 protects tumor cells from NK cell- and lymphokine-activated killer cell-mediated cytolysis. *J. Immunol.*, **168**, 2200–2211.
14. Goyos,A. *et al*. (2009) Novel nonclassical MHC class Ib genes associated with CD8 T cell development and thymic tumors. *Mol. Immunol.*, **46**, 1775–1786.
15. Flajnik,M.F. *et al*. (1993) A novel type of class I gene organization in vertebrates: a large family of non-MHC-linked class I genes is expressed at the RNA level in the amphibian *Xenopus*. *EMBO J.*, **12**, 4385–4396.
16. Goyos,A. *et al*. (2007) Involvement of nonclassical MHC class Ib molecules in heat shock protein-mediated anti-tumor responses. *Eur. J. Immunol.*, **37**, 1494–1501.
17. Edholm,E.S. *et al*. (2013) Nonclassical MHC class I-dependent invariant T cells are evolutionarily conserved and prominent from early development in amphibians. *Proc. Natl Acad. Sci. USA*, **110**, 14342–14347.
18. Goyos,A. *et al*. (2011) Remarkable conservation of distinct nonclassical MHC class I lineages in divergent amphibian species. *J. Immunol.*, **186**, 372–381.
19. Robert,J *et al*. (1994) Lymphoid tumors of *Xenopus laevis* with different capacities for growth in larvae and adults. *Dev. Immunol.*, **3**, 297–307.
20. Du Pasquier,L. *et al*. (1992) *In vitro* growth of thymic tumor cell lines from *Xenopus*. *Dev. Immunol.*, **2**, 295–307.
21. Robert,J. *et al*. (1997) Antibody cross-linking of the thymocyte-specific cell surface molecule CTX causes abnormal mitosis and multinucleation of tumor cells. *Exp. Cell Res*., **235**, 227–237.
22. Fisher,T.L. *et al*. (2002) Generation of monoclonal antibodies specific for human kallikrein 2 (hK2) using hK2-expressing tumors. *Prostate*, **51**, 153–165.
23. Nedelkovska,H. *et al*. (2010) Comparative *in vivo* study of gp96 adjuvanticity in the frog *Xenopus laevis*. *J. Vis. Exp.,* **43**, 2026.
24. Hallowes,R.C. *et al*. (1980) *A new dimension in the culture of breast*. Pergamon Press, Oxford and New York, pp. 215–245.
25. Morales,H.D. *et al*. (2010) Innate immune responses and permissiveness to ranavirus infection of peritoneal leukocytes in the frog *Xenopus laevis*. *J. Virol*., **84**, 4912–4922.
26. Robert,J. *et al*. (1998) Ontogeny of CTX expression in *Xenopus*. *Dev. Comp. Immunol.*, **22**, 605–612.
27. Nedelkovska,H. (2012) *Nonclassical MHC Class Ib Molecules: Critical Players in Tumor Immune Surveillance and Potential Immunotherapy Targets*. Ph.D. Thesis, Department of Microbiology and Immunology, School of Medicine & Dentistry, University of Rochester, Rochester, NY, pp. 212.
28. Wiendl,H. *et al*. (2002) A functional role of HLA-G expression in human gliomas: an alternative strategy of immune escape. *J. Immunol.*, **168**, 4772–4780.
29. Robert,J. *et al*. (2001) Phylogenetic conservation of the molecular and immunological properties of the chaperones gp96 and hsp70. *Eur. J. Immunol.*, **31**, 186–195.
30. Hix,L.M. *et al*. (2011) CD1d-expressing breast cancer cells modulate NKT cell-mediated antitumor immunity in a murine model of breast cancer metastasis. *PLoS One*, **6**, e20702.
31. Chiang,E.Y. *et al*. (2004) A nonclassical MHC class I molecule restricts CTL-mediated rejection of a syngeneic melanoma tumor. *J. Immunol*., **173**, 4394–4401.
32. Pilones,K.A. *et al*. (2012) Invariant NKT cells as novel targets for immunotherapy in solid tumors. *Clin. Dev. Immunol*., **2012**, 720803.
33. Cui,J. *et al*. (1997) Requirement for Valpha14 NKT cells in IL-12-mediated rejection of tumors. *Science*, **278**, 1623–1626.

*Received December 26, 2013; revised April 8, 2014;*
*accepted April 16, 2014*